Eddies in the Canada Basin, Arctic Ocean, Observed from Ice-Tethered Profilers

M.-L. TIMMERMANS, J. TOOLE, A. PROSHUTINSKY, R. KRISHFIELD, AND A. PLUEDDEMANN

Woods Hole Oceanographic Institution, Woods Hole, Massachusetts

(Manuscript received 23 February 2007, in final form 23 April 2007)

ABSTRACT

Five ice-tethered profilers (ITPs), deployed between 2004 and 2006, have provided detailed potential temperature θ and salinity S profiles from 21 anticyclonic eddy encounters in the central Canada Basin of the Arctic Ocean. The 12–35-m-thick eddies have center depths between 42 and 69 m in the Arctic halocline, and are shallower and less dense than the majority of eddies observed previously in the central Canada Basin. They are characterized by anomalously cold θ and low stratification, and have horizontal scales on the order of, or less than, the Rossby radius of deformation (about 10 km). Maximum azimuthal speeds estimated from dynamic heights (assuming cyclogeostrophic balance) are between 9 and 26 cm s^{-1}, an order of magnitude larger than typical ambient flow speeds in the central basin. Eddy θ–S and potential vorticity properties, as well as horizontal and vertical scales, are consistent with their formation by instability of a surface front at about 80°N that appears in historical CTD and expendable CTD (XCTD) measurements. This would suggest eddy lifetimes longer than 6 months. While the baroclinic instability of boundary currents cannot be ruled out as a generation mechanism, it is less likely since deeper eddies that would originate from the deeper-reaching boundary flows are not observed in the survey region.

1. Introduction

Eddies are known to be a common feature of the Canada Basin halocline having been observed in many past studies (Newton et al. 1974; Hunkins 1974; Manley and Hunkins 1985; D'Asaro 1988a; Padman et al. 1990; Plueddemann et al. 1998; Münchow et al. 2000; Muench et al. 2000; Krishfield et al. 2002; Pickart et al. 2005). The halocline layer lies above about 250-m depth in the Canada Basin and is characterized by a strong increase in salinity with depth and temperatures close to the freezing point (although incised by seasonal intrusions of warmer Pacific Ocean waters). Warmer, saltier water of North Atlantic Ocean origin occupies a layer below the halocline between about 250 and 800 m. The halocline effectively insulates the cold, fresh surface mixed layer (and thus the overlying sea ice) from the heat contained in the underlying Atlantic water. Eddies impact mixing and vertical heat transfer in the halocline, and, by trapping and transporting anomalous water, have implications for the lateral transport of heat, salt, and other water property anomalies within the Canada Basin.

Manley and Hunkins (1985) described 146 eddy encounters in the southern Canada Basin halocline from 14 months of drifting ice camp measurements [Arctic Ice Dynamics Joint Experiment (AIDJEX) in the Beaufort Sea 1975–76] and estimated that eddies could populate as much as 25% of the Beaufort Sea surface area. They showed that the mesoscale eddy component supplies the major amount of kinetic energy in the halocline. The vast majority of Manley and Hunkins's eddies were anticyclonic and were observed between 50 and 300 m. Manley and Hunkins hypothesized that the eddies formed as a result of instability of the Alaskan Coastal Current north of Point Barrow. D'Asaro (1988a) observed two anticyclones and two cyclones in the central Canada Basin, with the anticyclones centered on temperature maxima associated with halocline water of Pacific origin, and the deeper cyclones centered on temperature maxima associated with water of Atlantic origin, suggesting that the eddies were formed by instabilities of the Pacific and Atlantic water boundary currents, respectively. D'Asaro (1988b) showed that an important step in the generation of these eddies is a reduction in the potential vorticity of the origin water. He proposed that this occurs through the action

Corresponding author address: Mary-Louise Timmermans, WHOI, MS 21, Woods Hole, MA 02453.
E-mail: mtimmermans@whoi.edu

DOI: 10.1175/2007JPO3782.1

of frictional boundary torques that reduce the potential vorticity of the fluid as water from the Chukchi Sea flows through Barrow Canyon. However, observations of Münchow and Carmack (1997) and Pickart et al. (2005) indicated that horizontal current shears in the canyon are too small to support this mechanism of potential vorticity reduction.

During the Scientific Ice Expeditions (SCICEX) in 1997, Muench et al. (2000) performed a detailed survey of a cold-core anticyclone that was approximately 20 km in diameter and extended from 40 to 400 m deep. They used chemical tracers to place an upper limit of 2 yr on the age (i.e., the time since the waters were last in contact with the atmosphere) of the eddy. Pickart et al. (2005) observed similar cold-core anticyclonic eddies in the halocline over the continental slope north of Alaska. The eddies were centered around 100 m and were shown to have been formed by baroclinic instability of the Chukchi/Beaufort shelfbreak current (Pickart et al. 2005). Pickart et al. also suggested that the eddy surveyed by Muench et al. (2000) was likely formed by the same mechanism. The halocline eddies have long lifetimes. Padman et al. (1990) described a cyclonic eddy centered at a depth of 115 m in the central basin and inferred a decay time scale on the order of 10 yr, based on estimates of the rate of critical layer absorption of downward propagating internal wave momentum in a Canada Basin eddy.

Krishfield et al. (2002) analyzed observations of velocity in the Beaufort Sea halocline from the Ice-Ocean Environmental Buoy (IOEB) Program between 1992 and 1997. As in the AIDJEX study 20 yr previous (Manley and Hunkins 1985), sufficient numbers of eddies were observed to yield good statistics for eddy size, strength, and vertical structure. Krishfield et al. (2002) recorded 95 eddy encounters, most having core depths between 90 and 160 m and typical radii between 3 and 8 km. Maximum azimuthal speeds were 20–35 cm s^{-1}. They found an abundance of shallower eddies (center depths less than 80 m) over the Chukchi Plateau to the north and deeper eddies (core depths greater than 180 m) in the southern Canada Basin. It is possible that these two classes of eddies have different formation mechanisms and/or origin sites.

Here we present temperature and salinity measurements from an array of ice-tethered profilers (ITPs) in the Canada Basin. The observations show shallow anticyclonic eddies to be an important dynamical feature of the halocline. This is the first study of eddies in the central Canada Basin that extends as far north as 79°N, and it reveals shallower eddies likely having different origins than the more southern eddies of past studies. The eddies are characterized by local minima in temperature with a local minimum in buoyancy frequency N bounded by local N maxima above and below. They are centered near the top of the halocline at about 50-m depth, immediately below the surface mixed layer, and are about 25 m thick. Horizontal scales of the eddies are on the order of the Rossby radius of deformation or less (i.e., typical diameters of around 10 km or smaller).

In the next section, we describe the ITP array and observations. In section 3, we give an overview of the observed eddy characteristics and dynamics and highlight comparisons to eddies observed in past studies. We speculate as to a possible eddy generation site and formation mechanism in section 4. In section 5 we summarize our results and emphasize the need for future field experiments.

2. Observations

The ITP is an automated profiling CTD instrument that returns frequent high-vertical-resolution measurements of upper-ocean temperature and salinity beneath sea ice during all seasons for up to a 3-yr lifetime. A variant of the Woods Hole Oceanographic Institution (WHOI) moored profiler (Doherty et al. 1999), the ITP is designed to be deployed through a 10-inch-diameter ice hole drilled in multiyear ice that is several meters thick. The profiling vehicle is mounted to a tether and cycles vertically along it from just below the supporting ice floe to as deep as 800 m on a preprogrammed sampling schedule. The CTD on the ITP samples at 1 Hz and the vehicle profiles at a speed of about 25 cm s^{-1}, so that the raw data have a resolution of around 25 cm. Communication between the profiler and surface controller is by means of an inductive modem. The binary data are transmitted via satellite and acquired by a computer at WHOI. Data from the ITPs are unpacked and scaled immediately upon transmission (obvious errors are also removed) and made directly available on the Web (www.whoi.edu/itp). Technical details of the ITP system are given in Krishfield et al. (2006).

An array of five ITPs (Fig. 1) in the central Canada Basin has provided over 4000 profiles (as of November 2006) of temperature and salinity from 7–10 m down to 760-m depth. In August 2004, the first prototype ITP serial number 2 (ITP2) was deployed on a multiyear ice floe near 77°N, 141°W. A total of 243 profiles were obtained over 40 days (between 10- and 750-m depth) before the instrument stopped transmitting. Two more ITPs (serial numbers 1 and 3) were deployed in August 2005 at 79°N, 150°W (ITP1) and at 78°N, 142°W (ITP3). ITP3 returned via satellite four one-way temperature and salinity profiles (between 10- and 760-m depth) daily between August 2005 and September 2006.

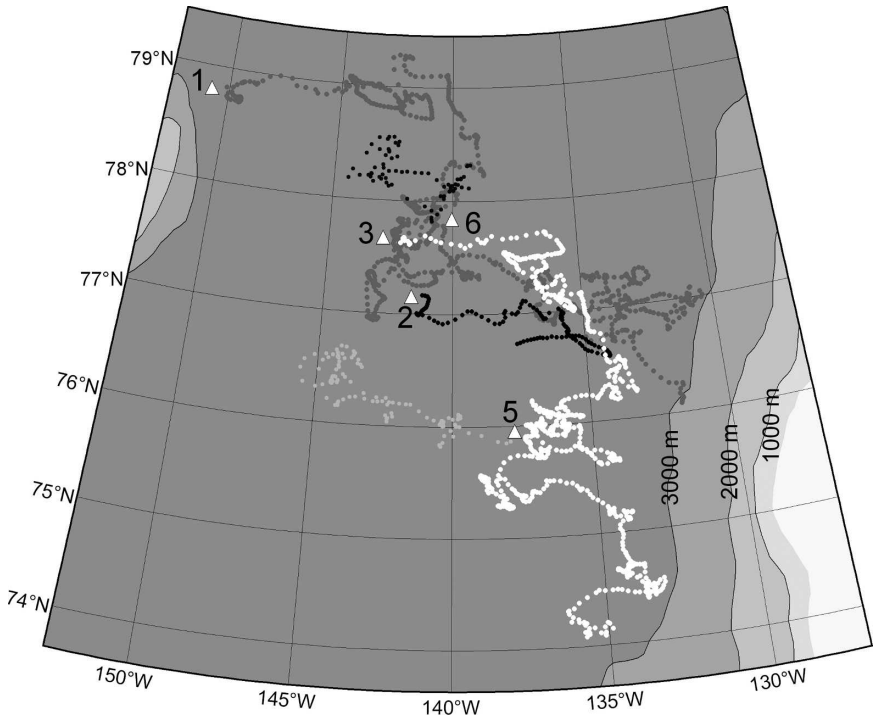

FIG. 1. Map of ITP drift tracks between 19 Aug 2004 and 16 Nov 2006. The instrument numbers and triangles mark the deployment positions.

ITP1 profiled and transmitted until January 2007 over the same depth range and on the same schedule as ITP3. After 2042 profiles, ITP1 stopped profiling because of a software bug (since fixed). ITPs 5 and 6 were deployed in September 2006 at 76°N, 138°W, and 78°N, 140°W, respectively, and both are presently reporting data. ITP5 (6) is returning three (two) one-way profiles of temperature and salinity between 7- (8-) and 760-m depth each day. We present an analysis of measurements taken from ITPs 1, 2, 3, 5, and 6 collected between 19 August 2004 and 16 November 2006 (a total of 1978 profiles since only the up-profiles have been used).

Profilers drift over the abyssal plain of the Canada Basin as the perennial ice pack moves (an anticyclonic gyre). Typical ice drift speeds are around 10–20 cm s^{-1}, an order of magnitude larger than typical upper-ocean current speeds in the Canada Basin. This implies a typical horizontal ITP survey resolution of about 3 km for up-profiles collected every 8–12 h. For the purposes of analyzing eddies with horizontal length scales on the order of 10 km, ITP drift surveys can be treated as synoptic.

3. Eddy properties

Between August 2004 and November 2006, there were 21 separate eddy encounters (Fig. 2), where an eddy encounter is defined on the basis of visual inspection of both potential temperature versus salinity diagrams and vertical sections, as discussed below. Profiles of potential temperature, salinity, and buoyancy frequency through a typical eddy (ITP3, 421) and outside the eddy (6 km to the northeast of the eddy center) show their vertical structure (Fig. 3). Table 1 gives characteristics of each eddy, which have been labeled according to the ITP profile number determined to be closest to the eddy center (see section 3a). Some of the variables listed in Table 1 are defined in Fig. 3.

Cross sections of potential temperature θ and salinity S (Figs. 4a,b) through a typical eddy (ITP3, 499) each show the convex lens shape indicative of anticyclonic flow. The eddies are located immediately below the surface mixed layer, centered between 42- and 69-m depth, and all eddies observed by ITPs have core waters that are anomalously cold relative to their surroundings. Buoyancy frequency is N (Fig. 4c), where $N^2 = -(g/\rho)(\partial\rho/\partial z)$, ρ is density, z is depth, and $g = 9.8$ m s^{-2}. Eddies are characterized by low stratification. Note that the reduced stratification of the eddies changes the effective stratification of the halocline and may be a preconditioning mechanism for higher heat fluxes through the halocline, which would in turn impact equilibrium ice thickness. Furthermore, the eddies are capped by a surface mixed layer, of thickness m −

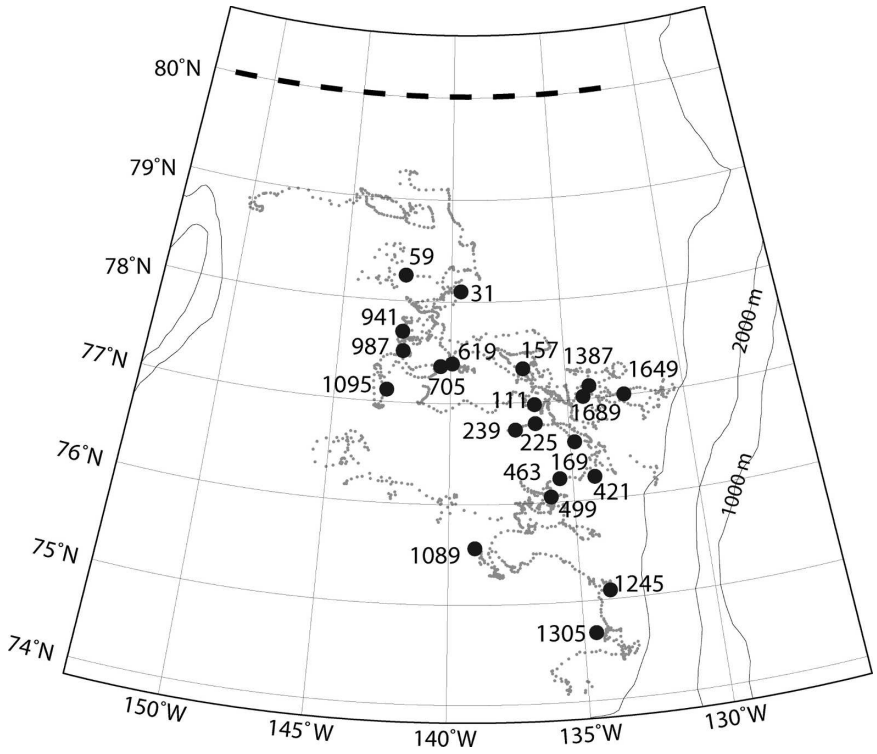

FIG. 2. Map of observed eddy locations (black dots) between 19 Aug 2004 and 16 Nov 2006. The numbers correspond to cast numbers closest to the eddy center, as given in Table 1. The dashed line at 80°N indicates the approximate location of the surface front discussed in section 4.

Δm (where m is the mixed layer thickness away from the eddy), that is typically around 30% shallower in the presence of an eddy.

a. Eddy azimuthal velocities and Rossby numbers

Eddy azimuthal velocities can be inferred from dynamic heights. Dynamic heights were computed for each eddy section, taking a reference level of 300 m (results are insensitive to vertical shifts of the reference level by 100 m). A balance between the pressure gradient, Coriolis, and centrifugal accelerations is considered (for an anticyclonic eddy, this cyclogeostrophic flow is faster than the geostrophic flow). That is,

$$\frac{v^2}{r} + fv - \frac{1}{\rho_0}\frac{\partial p}{\partial r} = 0,$$

where v is the cyclogeostrophic (gradient) velocity, p is the pressure, r is distance from the eddy center, ρ_0 is a reference density, and $f = 1.4 \times 10^{-4}\ \mathrm{s}^{-1}$ is the Coriolis parameter (Fig. 4d).

Visual inspection of the depth–distance sections (Fig. 4) indicates that eddy dimensions are approximately of the same order as the internal Rossby radius of deformation for the Arctic Ocean, $R_d = \sqrt{g'h}/f \approx 10$ km, where we have approximated the Arctic Ocean as a two-layer system, with the upper layer of thickness $h \approx 200$ m and density 1026 kg m^{-3} and the lower layer of density 1027.5 kg m^{-3} (see, e.g., Gill 1982). It is difficult to quantify exactly the horizontal extent of the eddies given that we do not know precisely how an ITP drifted relative to an eddy. However, we can estimate the core radius by assuming that the eddy is axisymmetric and has a core in solid-body rotation. This is a simple model eddy, known as a Rankine vortex, in which azimuthal velocity increases linearly with radius from zero to a maximum value $V = V_G$ at the outside edge $r = r_m$ of the core and falls off as $1/r$ outside r_m,

$$v(r) = \begin{cases} V_G r/r_m : r \le r_m \\ V_G r_m/r : r > r_m. \end{cases} \quad (1)$$

The Rankine vortex is the solution to a uniform potential vorticity anomaly (given by $2V_G/r_m$) within radius r_m. While the Rankine vortex structure is more simple than is expected for ocean eddies where, for example, the potential vorticity may not be completely uniform in the core, we will show that the model does capture the basic features of the flow. Further, for our purposes

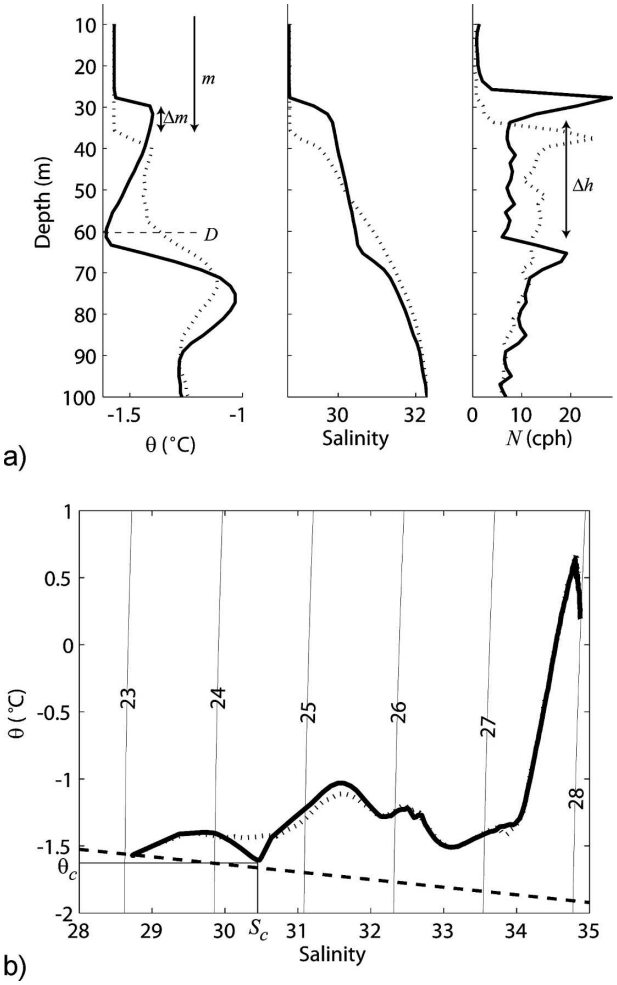

FIG. 3. (a) Two-meter-averaged profiles of potential temperature, salinity, and buoyancy frequency (computed over a 2-m interval) through a typical eddy (ITP3, 421). The dotted lines are profiles outside the eddy (6 km to the northeast of its center). (b) Potential temperature vs salinity for the same eddy. The dashed line is the freezing line at zero pressure, and lines of constant density (referenced to the surface) are also shown.

of estimating eddy core radii, we are not concerned that the velocity field outside r_m may have a slightly different profile than $1/r$.

We estimate eddy center positions as the point along each transect that is halfway between the locations of maximum and minimum estimated cyclogeostrophic velocity (at the middepth of the eddy) on opposite flanks of an eddy. These positions are only approximate because ITP profiles do not necessarily bracket r_m symmetrically on either side of an eddy.

For an axisymmetric eddy, if the ITP passes anywhere within the center half of the core, the error in the radius estimated by the half distance between the maximum and minimum cyclogeostrophic velocities will be only 15%. If estimated diameters are much less than R_d, we must assume that the ITP transected near the outside edge of an eddy core and its size cannot be estimated. In some cases, we observe an eddy feature based on a vertical profile, but the path of the ITP is such that there is insufficient evidence to estimate its size or azimuthal velocity. For 5 of the 21 eddy encounters, the ITP was found to transect at least within the center half of the core. Cyclogeostrophic velocities at the middepths of these five eddies as a function of distance from the estimated eddy center (Figs. 5a–e) indicate that the velocity appears to follow a linear relationship with r (solid-body rotation) within the core of an eddy, while outside the core the inverse relationship appears to be a reasonable approximation to the flow.

Table 1 gives radius r_m for each of the five eddies where the azimuthal velocity is a maximum $v = V_G$ (taken from the estimated eddy center), and Rossby number $\mathrm{Ro} = 2V_G/(r_m f)$. For the five eddies, $\mathrm{Ro} = -0.69 \pm 0.28$.

b. Comparison with past observations of eddies in the Canada Basin

The eddies observed in ITP measurements are typically shallower and less dense than eddies observed previously in the Canada Basin, with core densities of $\sigma \approx 24.6$ kg m^{-3} as compared with $\sigma \approx 26.5$ kg m^{-3} for previous observations (Fig. 6a). The majority of past studies have been confined to the southern and western Canada Basin, south of 75°N and west of 145°W, and the eddies observed were generally consistent with being formed from boundary current waters to the south. On the other hand, the ITP survey covers an area of the Canada Basin that is north of 74°N and east of 150°W (Fig. 6b). The differences in location and properties between the eddies suggest different source waters and/or formation mechanisms. It is noteworthy that the most spatially extensive of the past studies, that of Krishfield et al. (2002), revealed eddies that were smaller and shallower north of 76°N over the Chukchi Cap. The more northern ITP data are consistent with these findings, although Krishfield et al. (2002) have only velocity information for the eddies and so no θ–S comparisons can be made.

4. Eddy formation region and mechanism

The eddies we observe have core waters that are anomalously cold for the ITP sampling region, suggesting distant origins. Historical Canada Basin CTD and expendable CTD (XCTD) data reveal water having the same θ–S characteristics as the eddies outcropping to the surface mixed layer north of about 78°–80°N. The

TABLE 1. Estimated eddy parameters: cast refers to the ITP profile number determined to be closest to the eddy center, D is the depth of the potential temperature minimum θ_c, Δh is the eddy thickness, and Δm is the reduction in thickness (in meters) of the mixed layer (thickness m) under the eddy, as defined in Fig. 3. A dash for $\Delta m/m$ indicates that the mixed layer base was above the shallowest depth sampled by the ITP (note that this occurs each July). The S_c is the core salinity, and $\sigma_{\theta c}$ is the core potential density. Estimated maximum eddy azimuthal velocity V_G, radius r_m of maximum azimuthal velocity, and Rossby number Ro $[=2V_G/(r_m f)]$, where $f = 1.4 \times 10^{-4}$ s^{-1} is the Coriolis parameter, are also listed (computed in section 3a).

ITP	Cast	Date	D (m)	Δh (m)	$\Delta m/m$	θ_c (°C)	S_c	$\sigma_{\theta c}$ (kg m^{-3})	V_G (cm s^{-1})	r_m (km)	Ro
2	111	7 Sep 04	42	20	6/20	−1.49	30.22	24.29	—	—	—
2	169	16 Sep 04	65	24	6/21	−1.43	31.71	25.5	−26	3.8	0.98
2	225	26 Sep 04	44	22	6/24	−1.48	30.33	24.38	—	—	—
2	239	28 Sep 04	55	31	6/22	−1.59	30.79	24.75	—	—	—
1	619	17 Jan 06	55	29	6/20	−1.59	30.35	24.40	—	—	—
1	705	8 Feb 06	44	15	6/30	−1.49	30.21	24.28	—	—	—
1	941	8 Apr 06	46	12	4/22	−1.58	30.92	24.86	—	—	—
1	987	19 Apr 06	51	18	8/22	−1.59	30.97	24.90	−13	3.8	0.50
1	1095	16 May 06	55	18	8/22	−1.50	30.75	24.72	—	—	—
1	1387	28 Jul 06	51	18	—	−1.49	30.33	24.38	−10	2.3	0.62
1	1649	2 Oct 06	51	30	6/22	−1.44	29.70	23.87	−9	3.5	0.37
1	1689	12 Oct 06	69	33	6/26	−1.53	31.05	24.96	—	—	—
3	157	2 Oct 05	55	33	6/22	−1.60	30.46	24.49	—	—	—
3	421	7 Dec 05	61	29	9/34	−1.60	30.47	24.50	—	—	—
3	463	17 Dec 05	51	21	8/30	−1.51	30.08	24.18	—	—	—
3	499	26 Dec 05	50	24	10/28	−1.47	29.81	23.96	−20	2.9	0.99
3	1089	23 May 06	65	31	4/26	−1.62	31.28	25.15	—	—	—
3	1245	1 Jul 06	46	14	—	−1.40	29.87	24.00	—	—	—
3	1305	16 Jul 06	67	25	—	−1.37	31.3	25.16	—	—	—
6	31	20 Sep 06	61	35	6/24	−1.59	30.39	24.43	—	—	—
6	59	4 Oct 06	50	19	8/24	−1.47	30.11	24.20	—	—	—

Canada Basin north of 80°N is data sparse; however, the region was sampled during the SCICEX Program, which consisted of a series of scientific field operations using U.S. Navy submarines (data were available from the National Oceanographic Data Center at http://www.nodc.noaa.gov/). A north–south section of SCICEX XCTD data taken in October 2000 (Figs. 7, 8) shows a surface front between relatively warm freshwater to the south and colder, saltier surface water to the north. This front is likely associated with the northern edge of the Beaufort Gyre and the transpolar drift stream farther north. The mixed layer to the north is more characteristic of the Eurasian winter mixed layer (thicker than the Canadian winter mixed layer) with salinities in the range $30 < S < 31.5$ (see, e.g., Steele et al. 2004). The hatched region indicates water defined by a θ–S range of the observed eddy core properties ($\theta_c = -1.5 \pm 0.1$°C; $S_c = 30.5 \pm 0.5$). Representative θ–S curves from the northern and southern Canada Basin (Fig. 9), as well as through the core of an eddy, show the different surface water masses on either side of the front. SCICEX 1995–98 expeditions also reveal this front (Fig. 8). It seems more likely that the observed shift in frontal latitude is an interannual variation rather than seasonal. Proshutinsky and Johnson (1997) indicate shifts in Arctic Ocean circulation regimes (that appear to be forced by changes in the atmospheric circulation) that occur on time scales of about 5–7 yr. For example, during a positive North Atlantic Oscillation both the Beaufort Gyre and the transpolar drift stream weaken and move toward the Canadian Basin, which would result in a change in latitude of the front. Morison et al. (2006, 2007) have shown that since 2000, upper Arctic Ocean conditions have relaxed to pre-1990 conditions in response to a weakened North Atlantic Oscillation. That is, there has been a northward shift of the transpolar drift stream and the Beaufort Gyre boundary has extended north (i.e., a northward shift of the front). Note also that SCICEX 1999 does not show the front, but rather a salty surface layer as far south as 73°N. SCICEX 1995 and 1999 were April expeditions, whereas the other years were autumn expeditions.

The SCICEX CTD/XCTD profiles, which have a station spacing of about 50 km, allow us to estimate the alongfront geostrophic (baroclinic) flow relative to 300-m depth. For the SCICEX 1995–98 and 2000 sections, the geostrophic flow is between 3 and 5 cm s^{-1} (east) on the northern side of the front. This is similar to mean transpolar drift speeds of 2–4 cm s^{-1} (e.g., Rigor et al. 2002). The horizontal flow profile across the front meets necessary conditions for instability (f plane), leading to ageostrophic flows, because the value of the

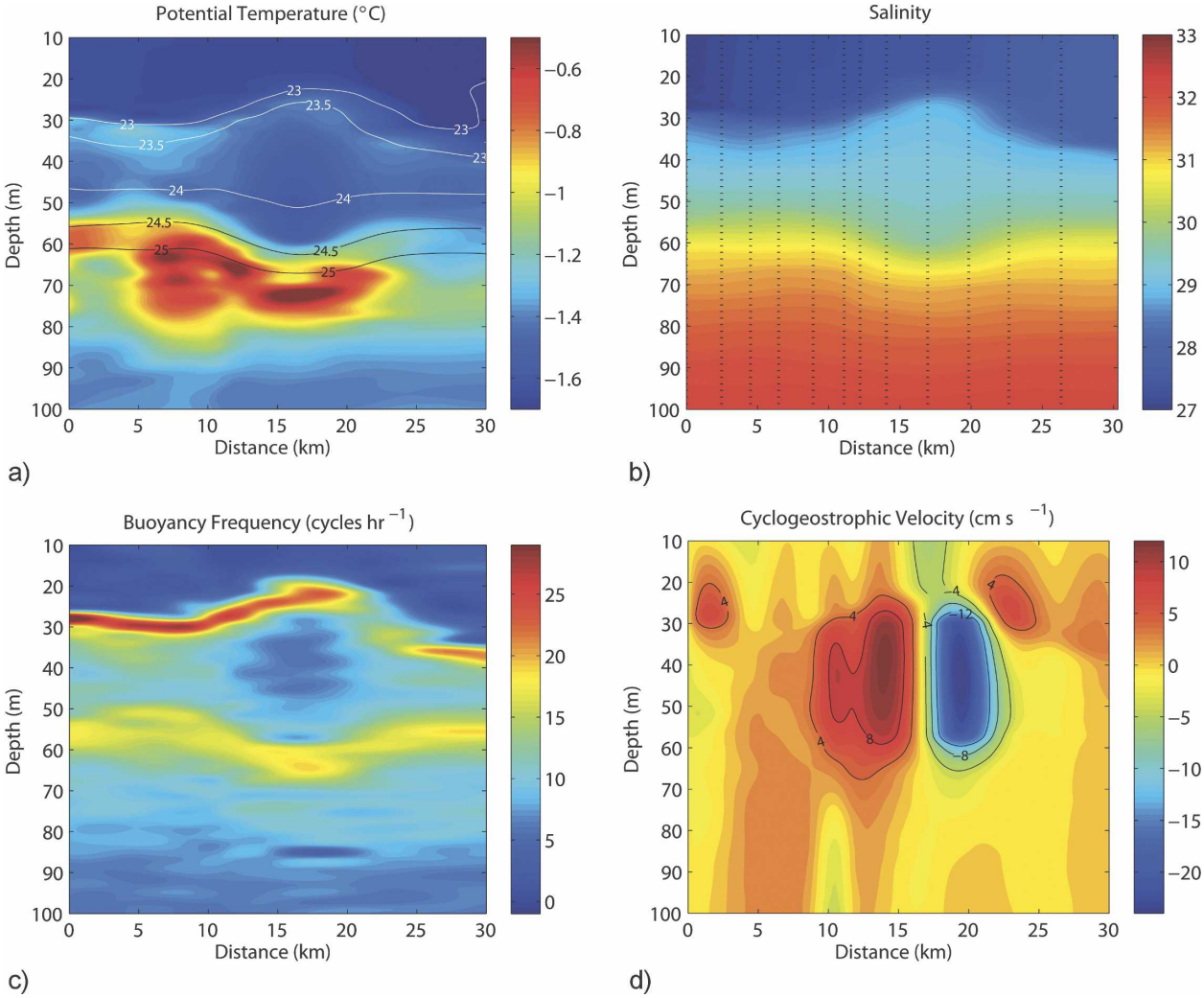

FIG. 4. Sections of (a) potential temperature, (b) salinity, (c) buoyancy frequency, and (d) cyclogeostrophic velocity through a typical eddy (ITP3, 499). Lines of constant potential density (referenced to the surface) are shown in (a). The section is from west (left) to east, and dotted lines in (b) indicate profile locations.

basic state vorticity gradient changes sign across the front. It is anticipated that future ITP instruments will cover the region of the Canada Basin north of 80°N, giving us more detailed information about the origin and variability of the surface water. Whatever the history of this water mass, it appears to be the source water for the observed eddies.

Spall (1995) formulated a mechanism for eddy formation by subduction at upper ocean fronts. When a surface geostrophic flow accelerates downstream, a compensating agestrophic cross-front flow is directed from the light side to the dense side of the front. The ageostrophic flow will be convergent on the dense side of the front, and, by conservation of mass, a deep cross-front flow will arise from the dense side to the light side in the subsurface layer below the front. Spall (1995) showed how parcels subducted from a deep surface layer will be characterized by anomalously low potential vorticity and anticyclonic circulation to compensate for compression (cyclonic circulation for shallow surface layers where the subducted parcels are stretched vertically). Spall assumes that the parcel of water originated on the dense side of the front with no relative vorticity and that the density and isopycnal potential vorticity are conserved as it is carried across the front; the thermal wind relation then requires that the subducted parcel be squashed and spread laterally as it develops a horizontal circulation (Fig. 10). He solves the equation of conservation of potential vorticity and the gradient wind relation for the thickness and azimuthal velocity of the resulting eddy.

The structure of the observed eddies is in agreement

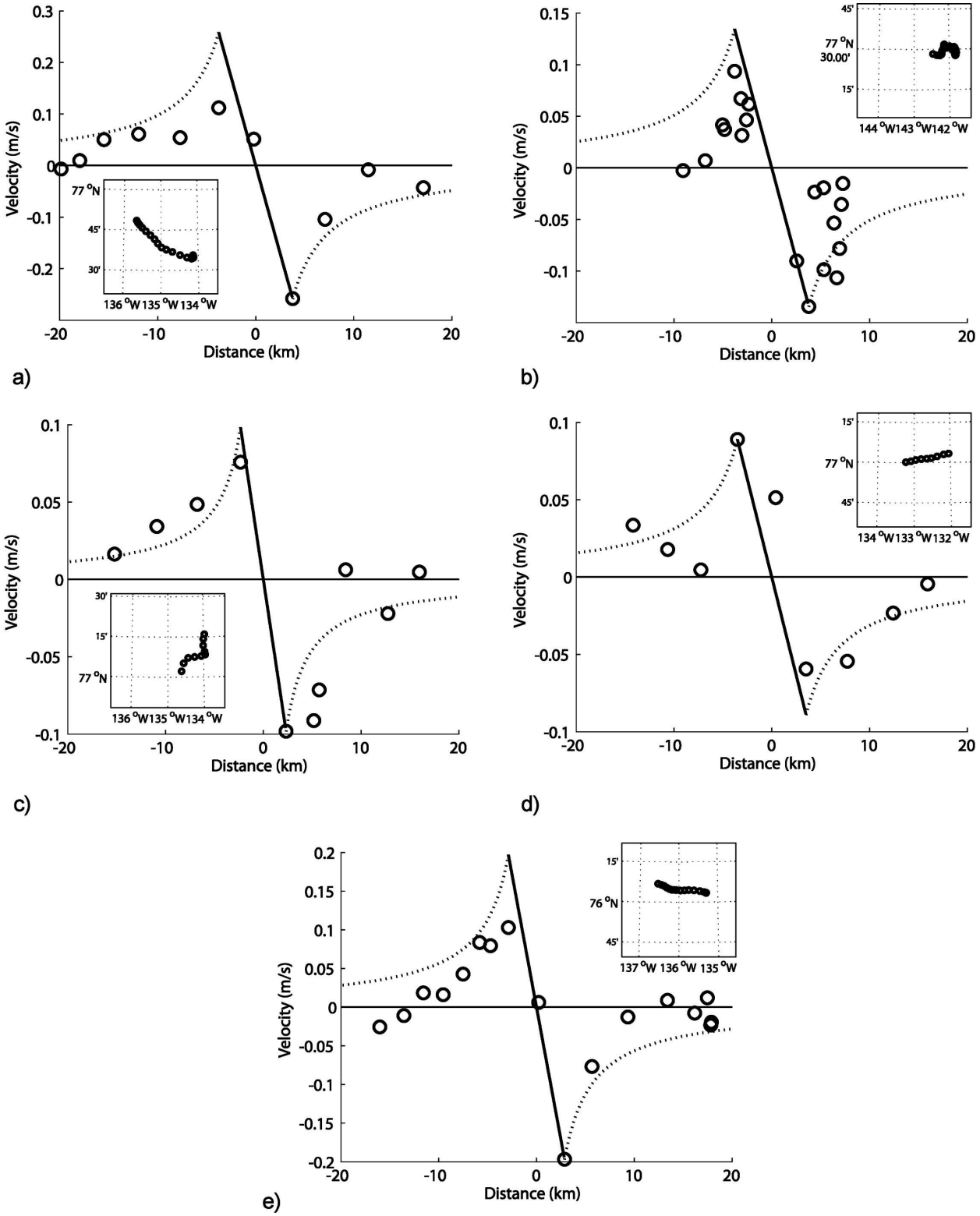

FIG. 5. Eddy cyclogeostrophic velocities (at the center depths) vs distance from the eddy center for eddies (a) 169, (b) 987, (c) 1387, (d) 1649, and (e) 499. Note that the vertical scale is not the same in (a)–(e). The solid curve corresponds to the Rankine vortex regime $r \leq r_m$, and the dotted curve corresponds to the regime $r > r_m$ given by Eq. (1).

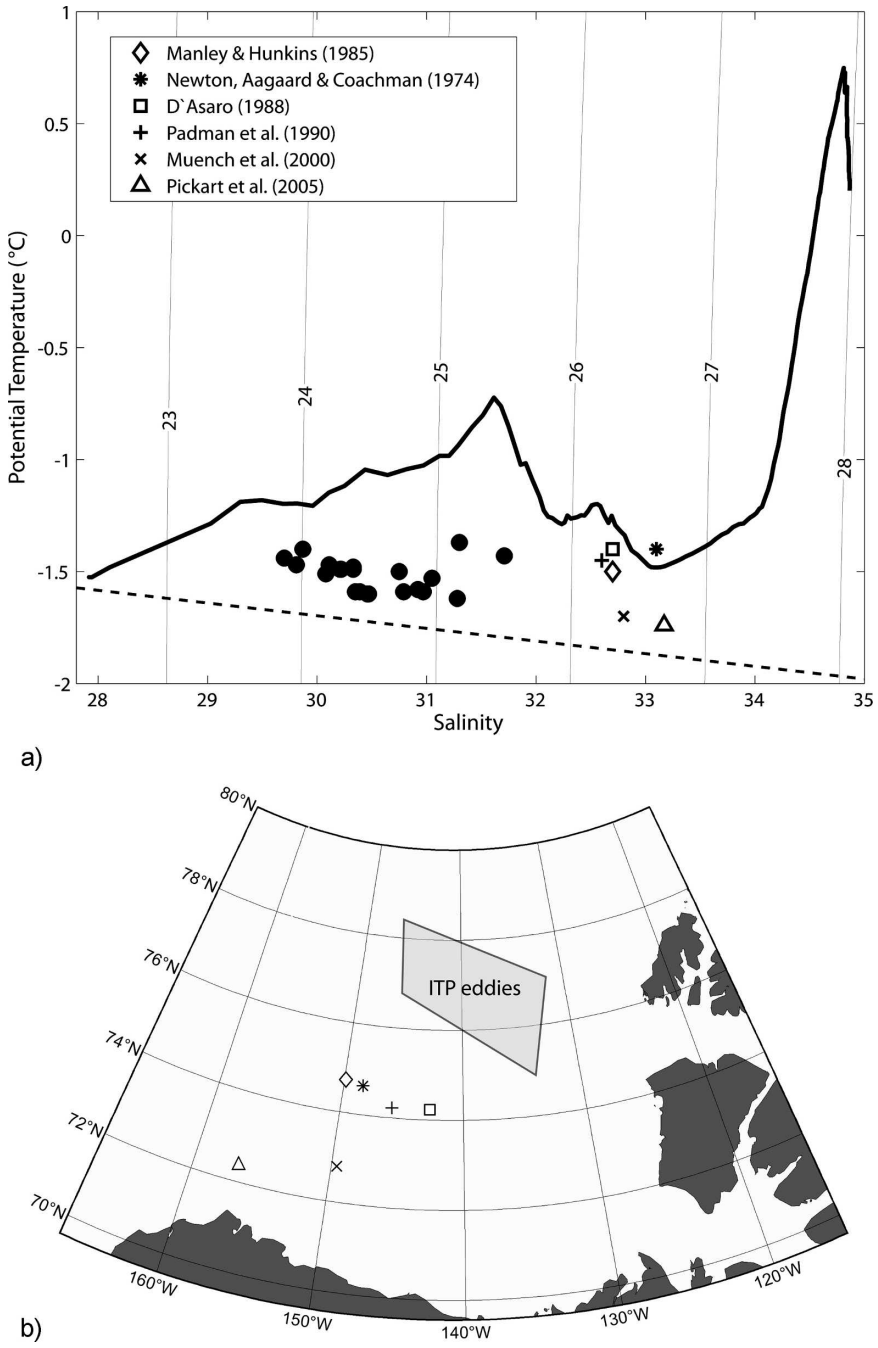

FIG. 6. (a) Potential temperature vs salinity in the Canada Basin. The solid curve shows a representative profile in the central Canada Basin (ITP3, profile 801; 76°N, 136°W; 12 Mar 2006). Dots mark the θ–S of the observed eddy cores, and the other symbols correspond to core properties of eddies observed previously in the Canada Basin. The dashed line is the freezing line at zero pressure, and lines of constant density (referenced to the surface) are also shown. (b) Location map of the eddies plotted in (a).

with Spall's model and appears to be consistent with their formation by instability of the observed surface front. The surface layer depth (on the dense side of the front, approximately the depth of the 25 kg m^{-3} isopycnal) is $h_m \approx 50$ m, while the thickness of the same isopycnal layer in the stratified interior (approximately the thickness of the 24–25 kg m^{-3} layer) is $h_i \approx 10$ m. The parameters are defined in Fig. 10.

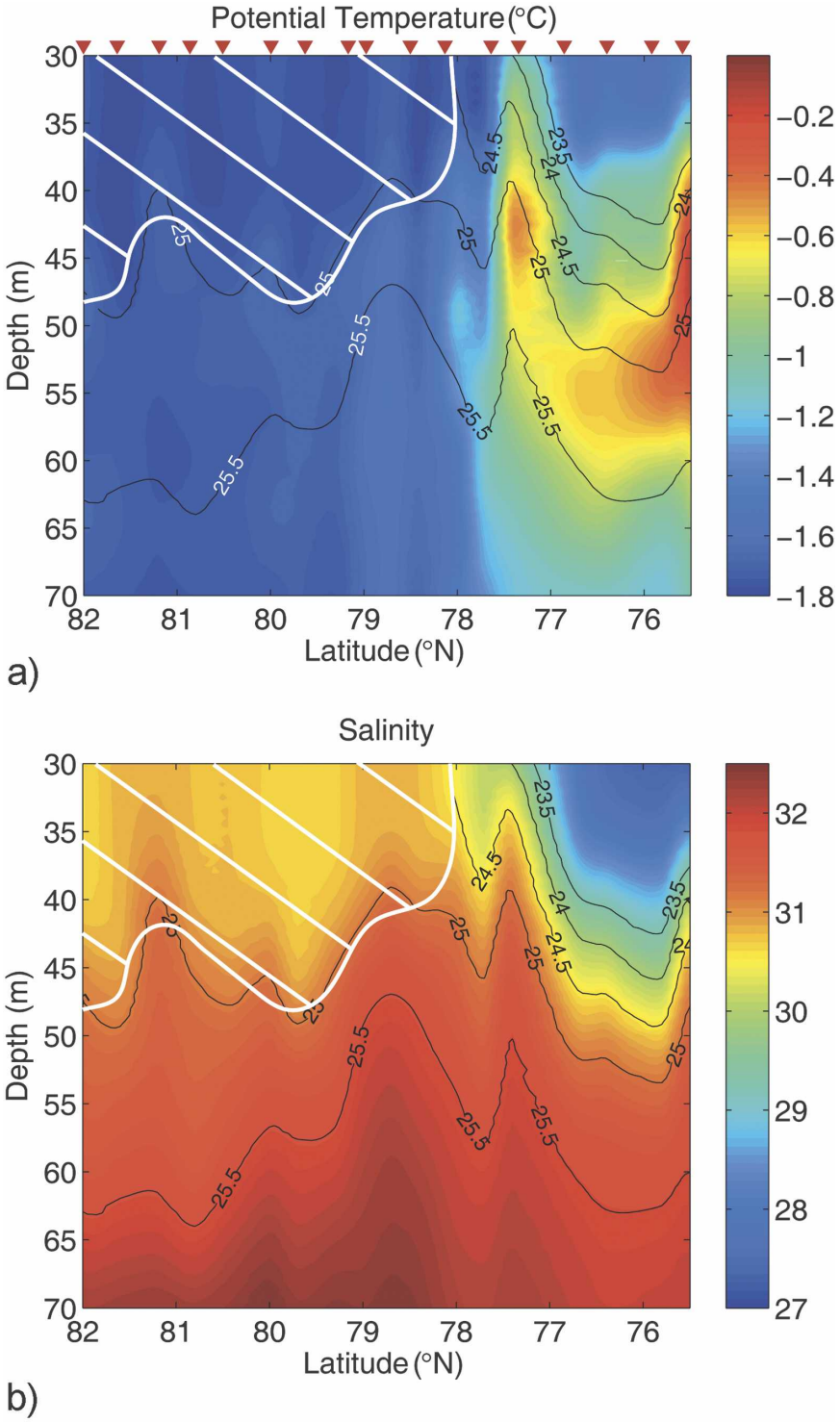

FIG. 7. North–south section of (a) potential temperature and (b) salinity from the SCICEX October 2000 expedition [the section track is shown in Fig. 8, and the red markers in (a) indicate XCTD profile locations]. Lines of constant potential density (referenced to the surface) are also shown. The hatched region indicates water defined by a θ–S range of the observed eddy core properties.

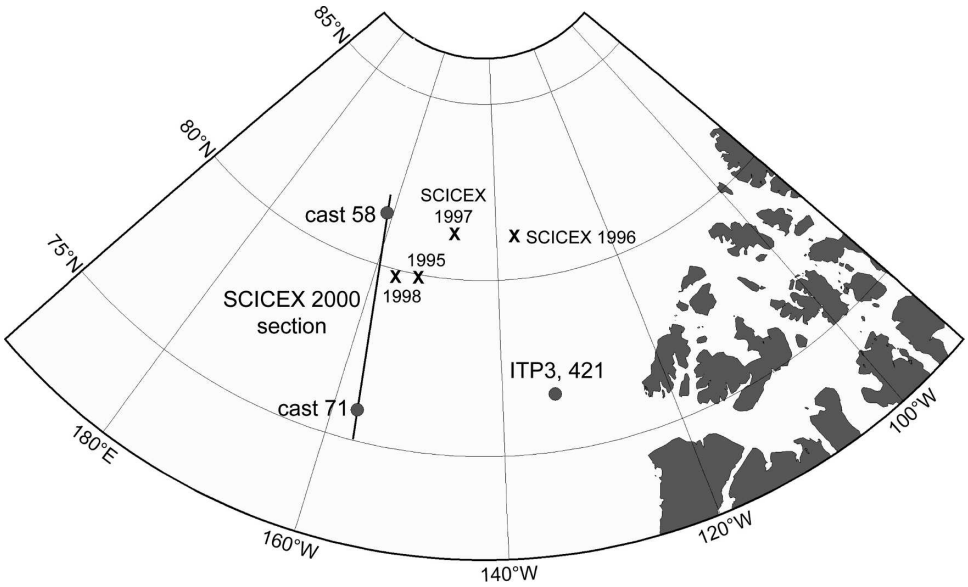

FIG. 8. Map showing the SCICEX 2000 section contoured in Fig. 7. Stations plotted in Fig. 9 are also shown. The location of the surface front as observed in other SCICEX expeditions is shown by an X.

Eddy core diameters are $r_m \approx 3$ km, giving a Burger number $B = g'h_m/(f^2 r_m^2) \approx 1$, where $g' \approx 0.01$ m s^{-2} is the reduced gravity across the front. For this B, h_m, and h_i, Spall's uniform potential vorticity solution predicts a thickness of the subducted parcel of $\Delta h \approx 16$ m and a relative vorticity $\zeta/f \approx -0.75$. These predictions are consistent with observed eddy thicknesses $\Delta h = 24 \pm 7$ m and Rossby numbers Ro $= -0.69 \pm 0.28$. Spall confirmed numerically that the structure of the resulting eddies is independent of the details of the subduction as long as potential vorticity is conserved during the process.

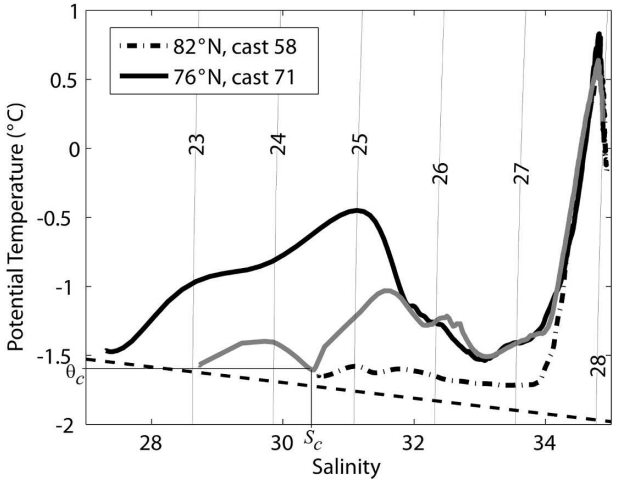

FIG. 9. Potential temperature vs salinity from SCICEX 2000 XCTD stations with locations shown in Fig. 8. The gray curve is a profile through eddy 421, ITP3. The dashed line is the freezing line at zero pressure. The core potential temperature θ_c and salinity S_c of the eddy are also marked.

5. Discussion

Our analysis of ITP measurements indicates that anticyclonic eddies are present in large numbers in the Arctic halocline north of 75°N in the Canada Basin. Approximately 10% of the most intensively ITP-sampled area of the Canada Basin (between about 76.8° and 77.7°N) is covered by shallow eddies, possibly having a significant impact on mixing and heat transfer in the halocline. Moreover, the eddies appear to have long lifetimes; a lower bound on eddy age can be deduced from the estimated time taken for it to travel 300–400 km from its possible generation site to its observed location in the central basin. If an eddy follows a straight path at an average speed of 1–2 cm s^{-1} (current measurements below the mixed layer in the central Canada Basin lie in this range; see www.whoi.edu/beaufortgyre/data_moorings.html), a minimum age of 6–18 months is obtained.

The structure of the cold-core anticyclones is consistent with their formation from water on the cold side of a zonal front that appears around 78°–80°N in historical XCTD and CTD surveys. Baroclinic instability of boundary currents seems less likely to be a generation mechanism for the cold, shallow eddies since deeper eddies that would originate from deeper boundary

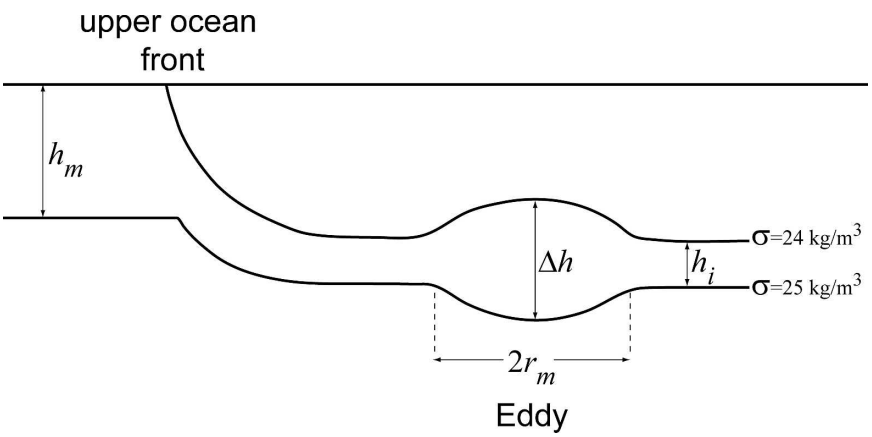

FIG. 10. Schematic cross section [similar to Fig. 1 of Spall (1995)] of the surface front showing the isopycnal layers and the subducted parcel that develops a horizontal circulation and becomes an anticyclonic eddy.

flows are not observed in the ITP survey region. Further, our analysis indicated no cyclonic eddies in the ITP measurements, which also lends support to the instability of a deep surface layer as the formation mechanism.

It is anticipated that future ITP deployments, in particular units equipped with velocity and dissolved oxygen sensors in addition to CTDs, will allow us to clearly define eddy azimuthal velocities, translation speeds, and formation sites and mechanisms so as to accurately assess their impact on property transports, mixing, and Arctic ice cover.

Acknowledgments. The engineering design work for the ITP was initiated by the Cecil H. and Ida M. Green Technology Innovation Program (an internal program at the Woods Hole Oceanographic Institution). Prototype development and construction were funded jointly by the U.S. National Science Foundation (NSF) Oceanographic Technology and Interdisciplinary Coordination Program and Office of Polar Programs (OPP) under Award OCE-0324233. Continued support has been provided by the OPP Arctic Sciences Section under Award ARC-0519899 and internal WHOI funding. Numerous WHOI engineers and technicians contributed to the ITP development and design, including Ken Doherty, Dan Frye, Terry Hammar, John Kemp, Don Peters, and Keith von der Heydt. We also acknowledge the technical assistance provided by McLane Research Laboratories, Inc., Sea-Bird Electronics, Inc., and Webb Research Corporation during the ITP development effort. We thank the officers and crew of the CCGS *Louis S. St-Laurent* and members of the science parties for their assistance in deploying the prototype instruments, as well as Eddy Carmack, Fiona McLaughlin, Sarah Zimmermann, and Koji Shimada for including our ITP activities in the collaborative Beaufort Gyre field program. Thanks also are given to Leif Thomas and Bob Pickart for valuable discussions.

REFERENCES

D'Asaro, E. A., 1988a: Observations of small eddies in the Beaufort Sea. *J. Geophys. Res.,* **93,** 6669–6684.

——, 1988b: Generation of submesoscale vortices: A new mechanism. *J. Geophys. Res.,* **93,** 6685–6693.

Doherty, K. W., D. E. Frye, S. P. Liberatore, and J. M. Toole, 1999: A moored profiling instrument. *J. Atmos. Oceanic Technol.,* **16,** 1816–1829.

Gill, A. E., 1982: *Atmosphere–Ocean Dynamics*. Academic Press, 662 pp.

Hunkins, K. L., 1974: Subsurface eddies in the Arctic Ocean. *Deep-Sea Res.,* **21,** 1017–1033.

Krishfield, R. A., A. J. Plueddemann, and S. Honjo, 2002: Eddies in the Arctic Ocean from IOEB ADCP data. Woods Hole Oceanographic Institution Tech. Rep. WHOI-2002-09, 144 pp.

——, and Coauthors, 2006: Design and operation of automated ice-tethered profilers for real-time seawater observations in the polar oceans. Woods Hole Oceanographic Institution Tech. Rep. WHOI-2006-11, 81 pp.

Manley, T. O., and K. Hunkins, 1985: Mesoscale eddies of the Arctic Ocean. *J. Geophys. Res.,* **90,** 4911–4930.

Morison, J., M. Steele, T. Kikuchi, K. Falkner, and W. Smethie, 2006: Relaxation of central Arctic Ocean hydrography to pre-1990s climatology. *Geophys. Res. Lett.,* **33,** L17604, doi:10.1029/2006GL026826.

——, J. Wahr, R. Kwok, and C. Peralta-Ferriz, 2007: Recent trends in Arctic Ocean mass distribution revealed by GRACE. *Geophys. Res. Lett.,* **34,** L07602, doi:10.1029/2006GL029016.

Muench, R. D., J. T. Gunn, T. E. Whitledge, P. Schlosser, and W. Smethie Jr., 2000: An Arctic Ocean cold core eddy. *J. Geophys. Res.,* **105,** 23 997–24 006.

Münchow, A., and E. C. Carmack, 1997: Synoptic flow and den-

sity observations near an Arctic shelf break. *J. Phys. Oceanogr.,* **27,** 1402–1419.

——, ——, and D. A. Huntley, 2000: Synoptic density and velocity observations of slope waters in the Chukchi and East-Siberian Seas. *J. Geophys. Res.,* **105,** 14 103–14 119.

Newton, J. L., K. Aagaard, and L. K. Coachman, 1974: Baroclinic eddies in the Arctic Ocean. *Deep-Sea Res.,* **21,** 707–719.

Padman, L., M. Levine, T. Dillon, J. Morison, and R. Pinkel, 1990: Hydrography and microstructure of an Arctic cyclonic eddy. *J. Geophys. Res.,* **95,** 9411–9420.

Pickart, R. S., T. J. Weingartner, L. J. Pratt, S. Zimmermann, and D. J. Torres, 2005: Flow of winter-transformed Pacific water into the western Arctic. *Deep-Sea Res. II,* **52,** 3175–3198.

Plueddemann, A. J., R. Krishfield, T. Takizawa, K. Hatakeyama, and S. Honjo, 1998: Upper ocean velocities in the Beaufort Gyre. *Geophys. Res. Lett.,* **25,** 183–186.

Proshutinsky, A. Y., and M. A. Johnson, 1997: Two circulation regimes of the wind-driven Arctic Ocean. *J. Geophys. Res.,* **102,** 12 493–12 514.

Rigor, I. G., J. M. Wallace, and R. L. Colony, 2002: Response of sea ice to the Arctic Oscillation. *J. Climate,* **15,** 2648–2663.

Spall, M. A., 1995: Frontogenesis, subduction, and cross-front exchange at upper ocean fronts. *J. Geophys. Res.,* **100,** 2543–2557.

Steele, M., J. Morison, W. Ermold, I. Rigor, M. Ortmeyer, and K. Shimada, 2004: Circulation of summer Pacific halocline water in the Arctic Ocean. *J. Geophys. Res.,* **109,** C02027, doi:10.1029/2003JC002009.